# Application of Microcontact Printing to Electroless Plating for the Fabrication of Microscale Silver Patterns on Glass

Chih-Hao Hsu, Ming-Chih Yeh, Kung-Lung Lo, and Li-Jen Chen*

*Department of Chemical Engineering, National Taiwan University, Taipei 10617, Taiwan*

*Received March 15, 2007. In Final Form: September 17, 2007*

Microcontact printing ($\mu$CP) and electroless plating are combined to produce microscale patterns of silver on glass substrates. Silver patterns with feature sizes of 0.6−10 $\mu$m stripes are fabricated using two methods. (1) The printing seeding layer (PSL) method is to apply $\mu$CP to directly print the catalyst Sn pattern for further electroless plating. (2) The printing masking layer (PML) method is to use $\mu$CP to print the octadecyltrichlorosilane (OTS) self-assembled monolayer as a masking layer on glass substrates, which then become Sn-activated in the unstamped regions by immersing the substrates in stannous chloride solution. After the electroless silver plating, the PML method has a better selectivity of silver deposition than the PSL method. In addition, variation of the deposited silver thickness as a function of the plating time and temperature is discussed.

## 1. Introduction

The feature size of circuits decreases substantially in the ultra-large-scale-integration (ULSI) technology. There are stringent demands on the quality of metal used for interconnects as well as the dimensions of these interconnect lines. Aluminum and copper are currently used for on-chip interconnects in the ULSI circuits. It is hard for aluminum to meet the requirement for the ever narrower and more densely packed interconnect lines due to its relatively high resistance. Although copper has a larger electrical conductivity, a lower electro-migration, and a lower stress migration, diffusion of copper into silicon is undesired, and a diffusion-barrier layer is thus required. To replace aluminum and copper in the ULSI circuits, silver is an ideal candidate for its relatively high melting point 962 °C and the highest electrical conductivity of all metals.

Silver can be deposited by electroless plating,[1a] electrochemical deposition, and physical vapor deposition. Electroless plating has attracted much attention in the microelectronics and semiconductor industries for its low processing temperature, low cost, high coverage, and uniform coating.[2−4] In addition, electroless plating can deposit metals or alloys on a variety of substrates without the need for a vaccum system.

Electroless plating is widely applied in the printed circuit board industry. Electroless plating is a plating process that involves deposition without any current applied, and the driving force for the reduction of metal ions is supplied by a chemical reducing agent in solution. Electroless plating is an autocatalytic redox process. The metal ion is reduced to metal only onto a surface, which must have a catalyst present for the reaction to begin with, and then the metal catalyzes its deposition.[1−6] Consequently, we can control the certain regions for metal deposition by selective seeding catalyst to substrate in the autocatalytic electroless plating.

Microcontact printing ($\mu$CP) is a soft lithographic technique for surface patterning,[7−9] and it triggers a new field in scientific research that has been rapidly growing over the past decade. $\mu$CP is based on transferring surface-reactive reagent (ink) from an elastomeric stamp to a substrate, and it enables one to fabricate remarkably accurate two-dimensional patterns down to the sub-micrometer scale. As compared to other processes, $\mu$CP has several potential advantages, such as simple procedure, low cost, and the deformability of the stamp, allowing it to accommodate rough surfaces.

Recently, $\mu$CP has been successfully applied to the electroless plating of metals (such as copper,[10−13] cobalt,[14] CdS,[15] and silver[16]) for surface patterning. $\mu$CP has been used to pattern dendrimer molecules acting as host templates for catalyst palladium. Electroless plating was then successfully conducted to deposit metals onto the regions of printed dendrimers.[12−15] On the other hand, Mewe et al.[16] used $\mu$CP to pattern an aminosilaned self-assembled monolayer for adhering gold nanoparticles as a catalyst for further electroless silver plating. There are some undesired silver depositions in the unstamped regions.[16] To prevent the undesired depositions for the electroless silver plating, in this study, $\mu$CP of a masking layer on glass is proposed, and

* Corresponding author. E-mail: ljchen@ntu.edu.tw.

(1) (a) *Electroless Plating: Fundamentals and Applications*; Mallory, G. O., Hajdu, J. B., Eds.; American Electroplaters and Surface Finisher Society: Orlando, FL, 1990. (b) Koura, N. In *Electroless Plating: Fundamentals and Applications*; Mallory, G. O., Hajdu, J. B., Eds.; American Electroplaters and Surface Finisher Society: Orlando, FL, 1990; Chaper 17.

(2) Lopatin, S.; Shacham-Diamand, Y.; Dubin, V. M.; Vasudev, P. K. In *Low and High Dielectric Constant Materials: Science, Processing and Reliability Issues*; Rathore, H. S., Singh, R., Thakur, R. P. S., Sun, S. C., Eds.; The Electrochemical Society Proceedings Series: Pennington, NJ, 1997; PV97-8, p 186.

(3) Shacham-Diamand, Y.; Inberg, A.; Sverdlov, Y.; Croitoru, N. *J. Electrochem. Soc.* **2000**, *147*, 3345.

(4) Okinaka, Y.; Osaka, T. In *Advances in Electrochemical Science and Engineering*; Gerisher, H., Tobias, C. W., Eds.; VCH: Weinheim, Germany, 1994; Vol. 3, p 58.

(5) Prissanaroon, W.; Brack, N.; Pigram, P. J.; Hale, P.; Kappen, P.; Liesegang, J. *Thin Solid Films* **2005**, *477*, 131.

(6) Dubin, V. M.; Shacham-Diamand, Y.; Zhao, B.; Vasudev, P. K.; Ting, C. H. *J. Electrochem. Soc.* **1997**, *144*, 898.

(7) Xia, Y. N.; Whitesides, G. M. *Angew. Chem., Int. Ed.* **1998**, *37*, 551.

(8) Huang, Z. Y.; Wang, P. C.; MacDiarmid, A. G.; Xia, Y. N.; Whitesides, G. M. *Langmuir* **1997**, *13*, 6480.

(9) Hidber, P. W.; Helbig, E.; Whitesides, G. M. U.S. Patent No. 6,060,121, 2000.

(10) Delamarche, E.; Geissler, M.; Magnuson, R. H.; Schmid, H.; Michel, B. *Langmuir* **2003**, *19*, 5892.

(11) Delamarche, E.; Vichiconti, J.; Hall, S. A.; Geissler, M.; Graham, W.; Michel, B.; Nunes, R. *Langmuir* **2003**, *19*, 6567.

(12) Bruinink, C. M.; Nijhuis, C. A.; Péter, M.; Dordi, B.; Crespo-Biel, O.; Auletta, T.; Mulder, A.; Schönherr, H.; Vancso, G. J.; Huskens, J.; Reinhoudt, D. N. *Chem.-Eur. J.* **2005**, *11*, 3988.

(13) Bittner, A. M.; Wu, X. C.; Kern, K. *Adv. Funct. Mater.* **2002**, *12*, 432.

(14) Wu, X. C.; Bittner, A. M.; Kern, K. *Langmuir* **2002**, *18*, 4984.

(15) Wu, X. C.; Bittner, A. M.; Kern, K. *Adv. Mater.* **2004**, *16*, 413.

(16) Mewe, A. A.; Kooij, E. S.; Poelsema, B. *Langmuir* **2006**, *22*, 5584.

10.1021/la7023988 CCC: $37.00 
Published on Web 10/18/2007

then the glass substrate becomes Sn-activated by immersing in stannous chloride solution. Tin is used as the catalyst, instead of gold, because tin can directly form covalent bonds to the glass surface.[17] That makes tin easy to be printed onto the glass substrate by using $\mu$CP. For comparison, $\mu$CP is also applied to pattern the seeding (Sn) layer directly on glass substrates. The electroless silver plating is then incorporated to produce selective microscale silver patterns on the Sn-activated regions of glass substrates. Good selectivity of the silver deposition is observed. The undesired silver deposition in the unactivated regions is dramatically eliminated by the method of the printing masking layer.

## 2. Experimental Section

**Materials.** Octadecyltrichlorosilane (OTS) and $H_2SO_4$ (98%) were obtained from Aldrich. $H_2O_2$ (30%) and dichloromethane (99%) were purchased from Merck. Polydimethylsiloxane (PDMS) SylgardTM184 was obtained from Dow Corning Co. 3,5-Diiodotyrosine (99%) and $AgNO_3$ (99.8%) were obtained from Acros. Potassium sodium tartrate tetrahydrate ($C_4H_4KNaO_6 \cdot 4H_2O$) (99.5%) and stannous chloride tetrahydrate ($SnCl_2 \cdot 2H_2O$) (99%) were obtain from Showa. Ethylenediamine was obtained from Tedia. All of these chemicals were used as received. Water was purified by double-distillation and then followed by a PURELAB Maxima Series (ELGA, LabWater) purification system with the resistivity always better than 18.2 M$\Omega$ cm. The microscope glass slides (FEA) were cleaned by piranha solution [a mixture 7:3 (v/v) of 98% $H_2SO_4$ and 30% $H_2O_2$] at 90 °C for 30 min before use.

**Electroless Silver Plating Solution.** The electroless plating solution is prepared according to ref 1. First, the complexing silver ion solution and the reducing agent solution are prepared separately. The complexing silver ion solution is composed of $3 \times 10^{-3}$ M silver nitrate and $1.8 \times 10^{-2}$ M ethylenediamine in 300 mL of aqueous solution. The reducing agent solution is composed of $3.5 \times 10^{-2}$ M Rochelle salt (potassium sodium tartrate) and $4 \times 10^{-5}$ M 3,5-diiodotyrosine in 700 mL of aqueous solution.[1b] These two solutions are then well mixed to form the electroless plating solution just right before the silver plating. In addition, the plating bath is carried out at a prescribed temperature, and its pH value always falls between 10 and 10.5 during the process of electroless plating.

**Fabrication of Silver-Patterned Glass Substrates.** Microcontact printing incorporated with electroless plating is applied to generate silver patterns on glass substrates by using two different methods: (1) printing seeding layer (PSL) and (2) printing masking layer (PML).

The PSL method is schematically illustrated in Figure 1. For the PSL method, the stannous chloride ($SnCl_2$) solution is used as the printing ink to apply onto the PDMS stamp, which is dried by nitrogen stream. The $SnCl_2$ solution is composed of 50 mL of water, 0.5 mL of 18 M hydrochloric acid, and 0.5 g of $SnCl_2 \cdot 2H_2O$.[1] The PDMS stamp is then brought into conformal contact with the surface of a glass substrate for 15 min to print the seeding layer. After $\mu$CP, a very reproducible amount of tin is left on the stamped areas of the glass substrate as a chlorine-free compound.[17] That is, the stamped areas become Sn-activated. This Sn-seeded glass substrate is then immersed into the electroless plating solution for a prescribed time period at a constant temperature. The silver pattern is then generated right at the Sn-activated (or stamped) regions.

On the other hand, Figure 2 illustrates the schematic procedure of the PML method. For the PML method, the OTS solution, instead of the $SnCl_2$ solution, is applied as the ink to the $\mu$CP to pattern a masking OTS self-assembled monolayer (SAM) on the glass substrate. The OTS solution is composed of 10 mL of dehydrated isooctane and 3.5 $\mu$L of OTS. It is well understood that chlorosilanes are very sensitive to the environmental humidity.[18] Note that this $\mu$CP is performed in a glovebag filled with dry nitrogen to exclude

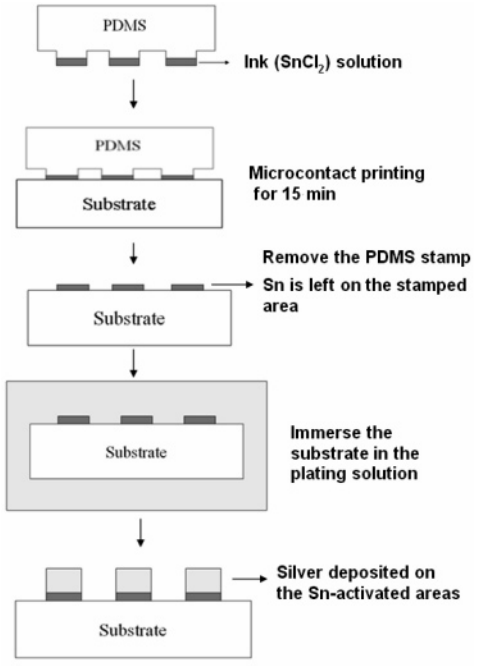


**Figure 1.** Schematic illustration of the printing seeding layer method.

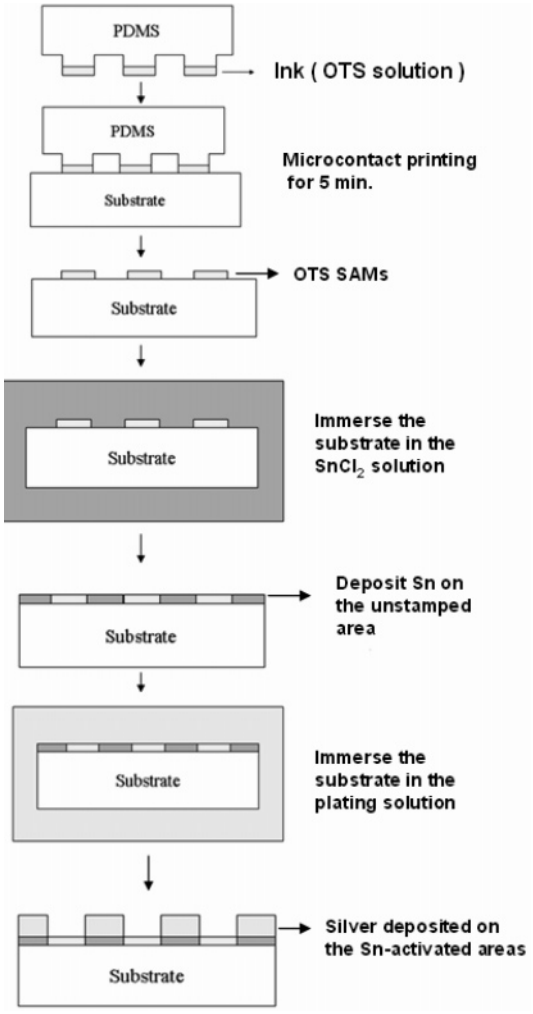


**Figure 2.** Schematic illustration of the printing masking layer method.

the amount of water traces in the surrounding atmosphere. This glass substrate with the patterned masking layer is further immersed in the $SnCl_2$ solution to deposit the catalyst Sn onto the unstamped

(17) De Minjer, C. H.; v. d. Boom, P. F. J. *J. Electrochem. Soc.* **1973**, *120*, 1644.

(18) Chen, L.-J.; Tsai, Y.-H.; Liu, C.-S.; Chiou, D.-R.; Yeh, M.-C. *Chem. Phys. Lett.* **2001**, *346*, 241.

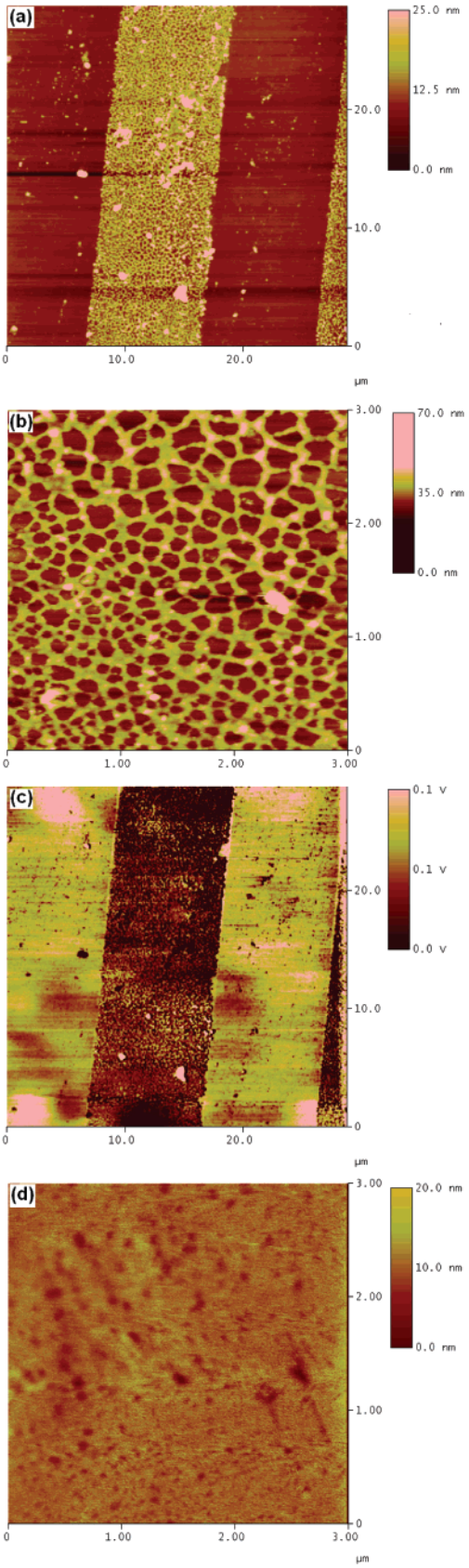


**Figure 3.** The AFM images of the Sn-activated area prepared by the PSL method (a−c) and by the PML method (d). (a) Image size, 30 $\mu$m × 30 $\mu$m; (b) image size, 3 $\mu$m × 3 $\mu$m; (c) friction force image of image (a); and (d) image size, 3 $\mu$m × 3 $\mu$m.

regions of the glass substrate. When the substrate is removed from the $SnCl_2$ solution, the substrate is rinsed with water several times

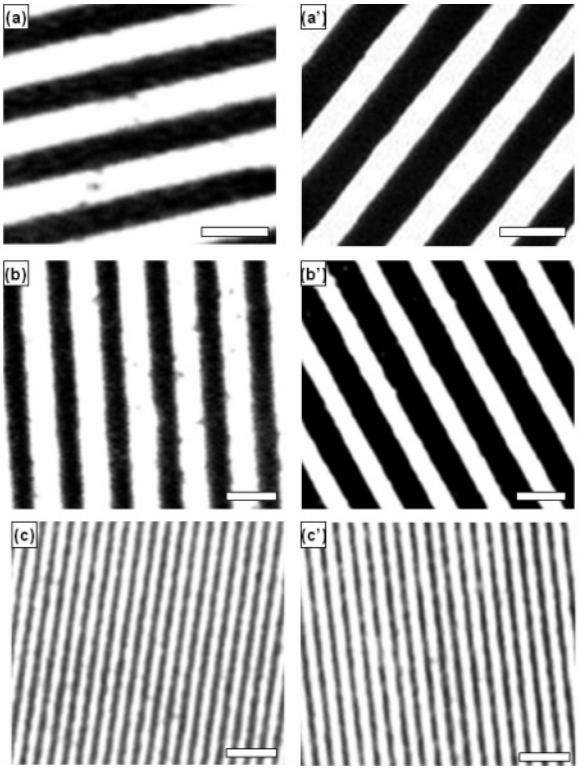


**Figure 4.** Optical micrographs of silver stripe patterns fabricated by the PSL method [shown in the left column: (a−c)] and by the PML method [shown in the right column: (a′−c′)]: (a) and (a′) parallel stripe pattern with a line width 10 $\mu$m and a period 20 $\mu$m, scale bar = 20 $\mu$m; (b) and (b′) parallel stripe pattern with a line width 2 $\mu$m and a period 4 $\mu$m, scale bar = 4 $\mu$m; (c) and (c′) parallel stripe pattern with a line width 0.6 $\mu$m and a period 1.2 $\mu$m, scale bar = 4 $\mu$m.

and blown dry by nitrogen gas. Electroless silver plating is then carried out by immersing the substrate in the plating bath for a prescribed time period at a constant temperature. The silver pattern is then generated right at the Sn-activated (or unstamped) regions.

The contact mode atomic force microscope (AFM, Nanoscope IIIa, Digital Instrument, Santa Barbara) is then used to explore the surface topography of the silver patterned surfaces. Silicon nitride tips (Digital Instrument) with a spring constant of 0.06 N/m are used to image samples under ambient condition.

## 3. Results and Discussion

Microcontact printing is applied to fabricate the parallel stripe pattern of the Sn-activated glass substrates with a line width of 10 $\mu$m and a period of 20 $\mu$m. Figure 3 shows the AFM images of the Sn-activated surfaces fabricated by the PSL method and by the PML method before the electroless plating. It is interesting to note that the Sn-activated area resulting from the direct printing seeding layer generates an irregular network-like pattern on the glass substrate, as shown in Figure 3a and b. Note that the holes of irregular network-like pattern on the Sn-activated area have exactly the same height as the bare glass area, as shown especially in Figure 3b. It is believed that there is no Sn deposited on these holes. It can be further confirmed by the friction force image of Figure 3a, as shown in Figure 3c, which demonstrates that the holes of irregular network-like pattern on the Sn-activated area have the same friction force as the bare glass surface. On the other hand, one cannot observe the network-like pattern in the Sn-activated area resulting from the immersion in $SnCl_2$ solution (the printing masking layer method), as illustrated in Figure 3d. In other words, the morphology of the Sn-activated surfaces is quite different between the surfaces fabricated by the PSL method

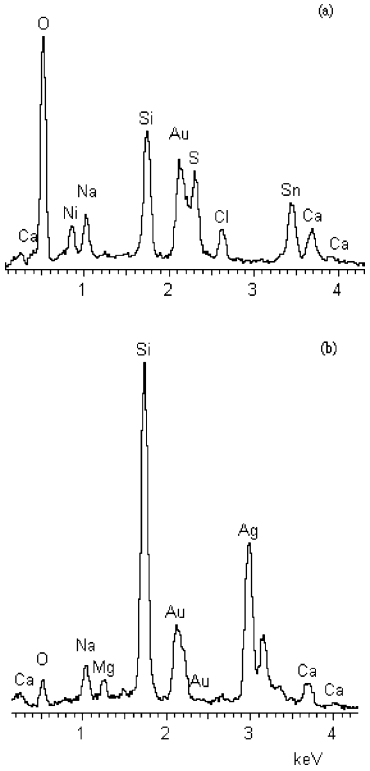


**Figure 5.** The EDX spectrum for the glass substrate with the Sn-seeding layer fabricated by the PML method (a) before and (b) after the electroless silver plating.

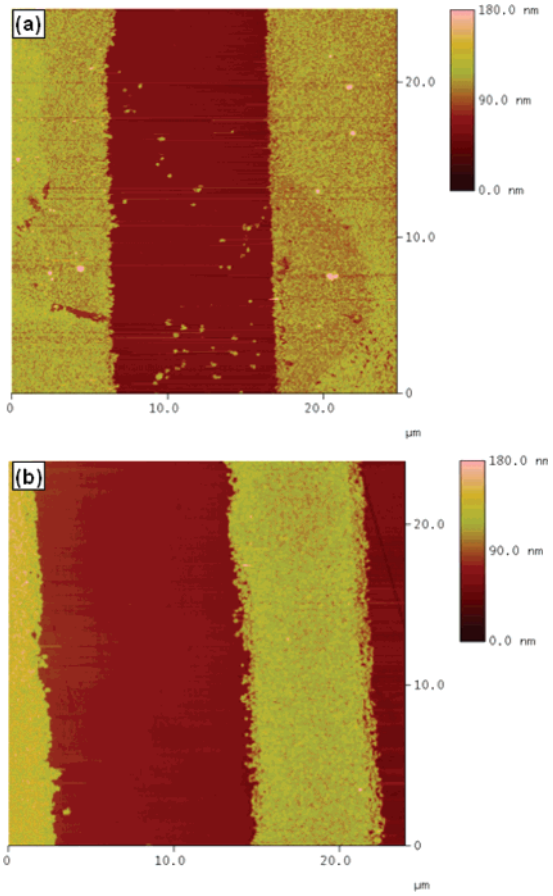


**Figure 6.** AFM images of silver pattern fabricated (a) by the PSL method and (b) by the PML method.

and by the PML method before the electroless plating. However, the morphology of the silver pattern on the Sn-activated surfaces

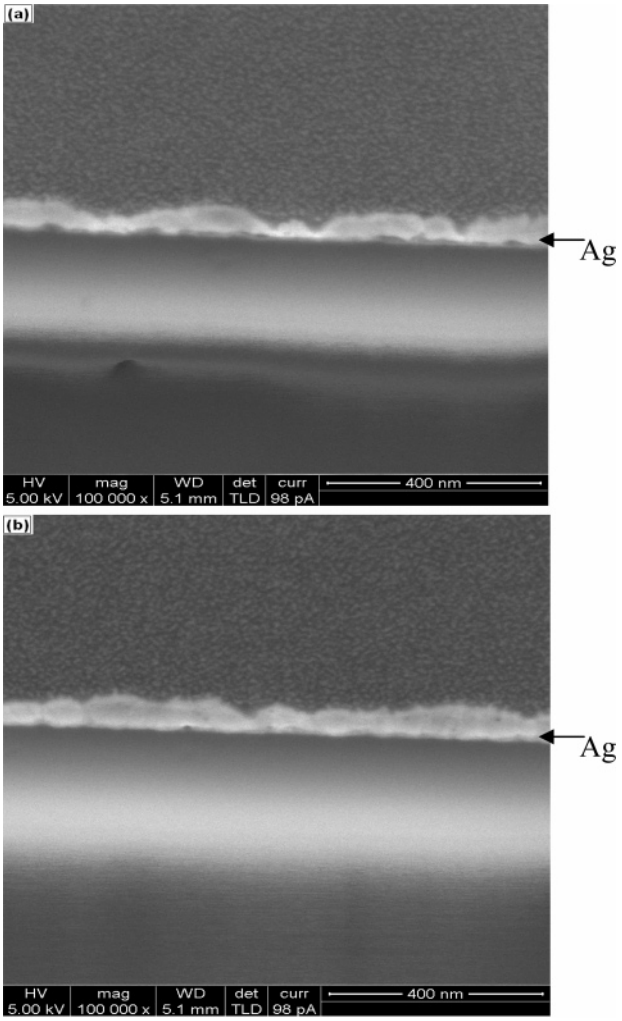


**Figure 7.** The cross-sectional SEM images of the silver pattern fabricated (a) by the PSL method and (b) by the PML method.

becomes identical for these two methods after the electroless plating. We will come back to this point later. Note that some Sn-islands appeared in the unstamped area of the substrate fabricated by the PSL method, as shown in Figure 3a. The friction force image, Figure 3c, also consistently illustrates the existence of the Sn-islands in the unstamped area of the substrate. It is expected that these unexpected Sn-islands would introduce unwanted silver depositions besides the stamped Sn-activated area after the electroless plating.

These Sn-activated patterned substrates are then immersed in the plating solution to conduct the electroless silver plating at 45 °C for 4 min. Figure 4 shows the optical micrographs (Olympus, BXFM) of the silver patterns at three different line widths fabricated by the PSL method and by the PML method. The left column of Figure 4 illustrates the results of the PSL method and the right column for that of the PML method. The white stripes are the region of the deposited silver. It is obvious that both the PSL and the PML methods have good selectivity of silver deposition. As one can see in Figure 4b and b′, the edge of the silver stripes of the PML method is sharper than that of the PSL method. More precisely, the selectivity of the PML method is slightly better than that of the PSL method. To further verify this point, the AFM is applied to explore the surface topology of these silver patterned surfaces.

The EDX spectrum of the Sn-activated area before the electroless silver plating shown in Figure 5a confirms the presence

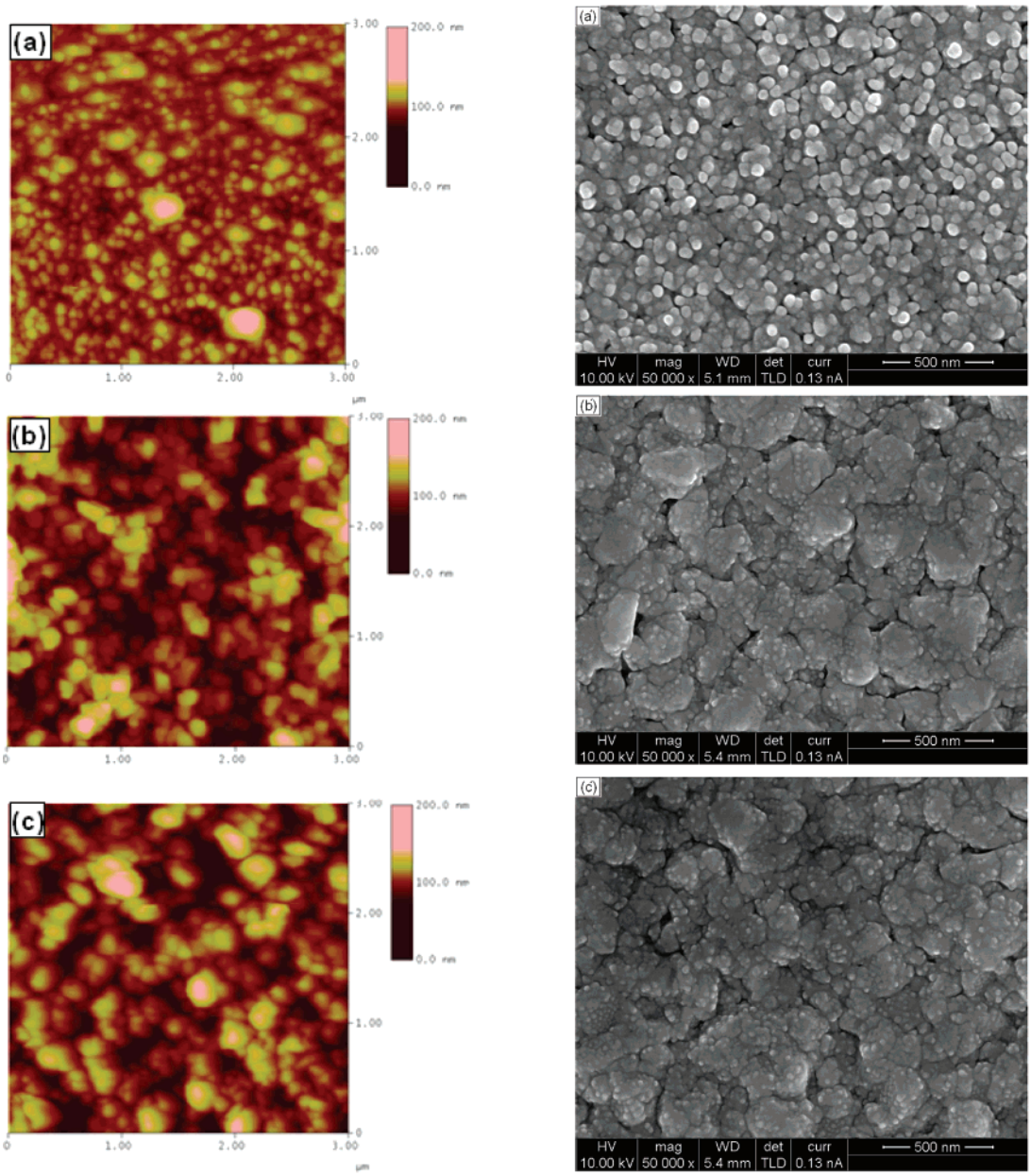


**Figure 8.** AFM (left column) and SEM (right column) images of silver pattern under the condition of the plating time of 4 min (a and a′), 30 min (b and b′), and 60 min (c and c′) at 45 °C. AFM image size: 3 $\mu$m × 3 $\mu$m. The substrates are fabricated by the PML method.

of deposited Sn. After the electroless silver plating, the EDX spectrum of the silver stripe shown in Figure 5b verifies the presence of metallic silver. Note that the signal of Sn is too weak to be identified in Figure 5b.

Figure 6a and b illustrates the AFM images of silver pattern fabricated by the PSL method and by the PML method, respectively. It is obvious, as shown in Figure 6a, that some silver particles appeared in the unstamped area of the substrate fabricated by the PSL method. The existence of the undesired silver particles is due to the unexpected Sn deposition in the unstamped area during the process of $\mu$CP for the PSL method, as mentioned above. The friction force image (not shown) also confirms that those small grains in the unstamped area (by the PSL method) are silver particles. On the other hand, there are almost no silver particles deposited in the area of the OTS-SAM masking layer of the substrate fabricated by the PML method, as shown in Figure 6b. The OTS-SAM masking layer does prevent the surface from silver deposition. It is a direct evidence that the OTS-SAM masking layer is very effectively excluded from the Sn-activation when the glass substrate with the patterned masking layer is immersed in the $SnCl_2$ solution to deposit the catalyst Sn onto the unstamped regions of the bare glass substrate in the process of the PML method.

It is essential that the silver strip is continuous for being the interconnect lines in integrated circuit. One may suspect the continuity of the silver strip by simply examining the AFM images, as shown in Figure 6. The cross-sectional SEM images of the silver pattern fabricated by the PSL method and by the PML method are shown in, respectively, Figure 7a and b, which verify the continuity of the silver stripe. In addition, one can observe that the silver pattern fabricated by the PML method is more uniform than the one fabricated by the PSL method. This less uniform pattern fabricated by the PSL method may be attributed to the irregular network-like pattern of Sn in the $\mu$CP process, as shown in Figure 3b. On the other hand, the Sn-seeding layer resulting from the PML method is more uniform, as shown in Figure 3d, which leads to better uniformity of the silver stripe.

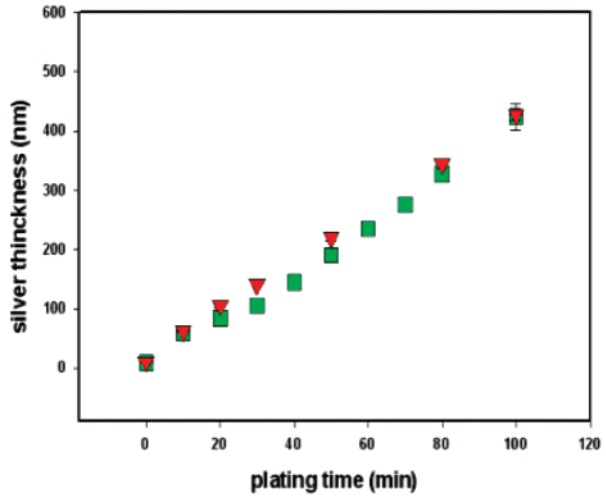


**Figure 9.** Variation of the silver thickness as a function of the plating time for the substrates fabricated by the PSL (green ■) method and by the PML (red ▼) method.

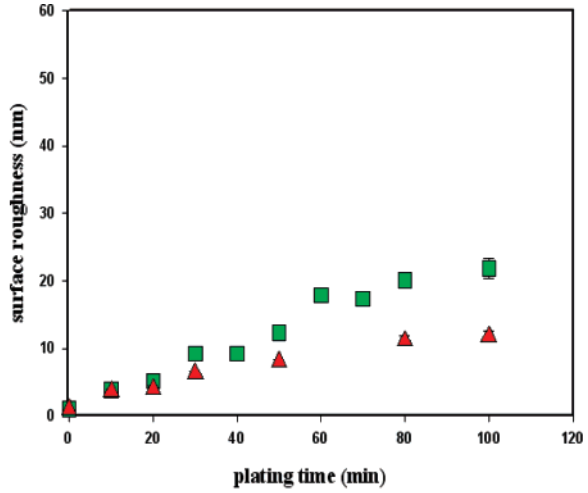


**Figure 10.** Variation of the surface roughness of the Sn-seedless region as a function of the plating time for the substrates fabricated by the PSL (green ■) method and by the PML (red ▲) method.

To further examine the continuity of the silver stripes, the conductivity of the silver stripes is measured by using the four-point probe method (Agilent 4338B Milliohmmeter). The silver stripes are prepared by using the PML method, and a conductivity of $44 \times 10^6$ S/m is measured. This value is lower than the bulk conductivity of silver, $63 \times 10^6$ S/m. The conductivity of the silver film is subject to grain boundary and defects.

As one can see in Figure 6, the silver deposition is granular. Figure 8 presents the zoom-in AFM and SEM images of the silver depositions for three different plating times, 4, 30, and 60 min, at 45 °C prepared by the PML method. The silver grain size is 138(±17) nm for the plating time of 4 min, as shown in Figure 8a. The standard deviation of the grain size is given in the parentheses. The grain size increases along with the plating time. The grain size is increased up to 303(±34) nm [Figure 8b] for the plating time of 30 min, and 349(±71) nm [Figure 8c] for 60 min plating time. It should be noted that the variation of the grain size increases along with the plating time, as one can tell from the standard deviation of the grain size. The surface roughness of the deposited silver pattern can be further determined directly from these AFM images.

It is obvious to see the morphology of the deposited silver pattern varies along with the plating time, as one can see from the SEM images in Figure 8a′, b′, and c′. When the plating time is short, say 4 min, the deposited silver is granular and round, as shown in Figure 8a′. When the plating time is increased, the granular silver agglomerates to form a larger and irregular shape aggregate. Note that there are small round grains growing on top of these large aggregates, as demonstrated in Figure 8b′ and c′.

The silver thickness can be further determined by the AFM. Because both surface areas of the silver pattern regions and of the Sn-seedless regions are rough, the deposited silver thickness is then defined as the difference between the average height of the silver pattern regions and that of the Sn-seedless regions. The variation of the silver thickness as a function of the plating time for both the PSL and the PML methods at 45 °C is shown in Figure 9. The silver thickness linearly increases along with the plating time, consistent with the result of Koura.[1b] The growth rate of the silver thickness for the electroless plating is about 4.3 nm per min. There is no significant thickness difference between the results obtained by the PML method and the PSL method.

Note that there are some unexpected Sn-depositions in the unstamped regions in the process of the $\mu$CP for the PSL method,

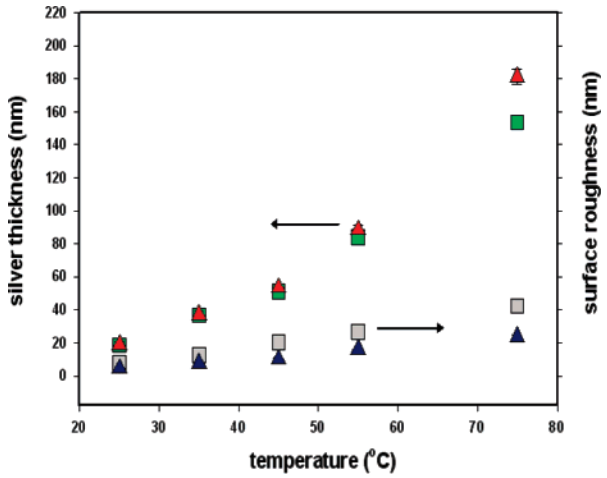


**Figure 11.** Variation of the silver thickness and surface roughness of the deposited silver pattern as a function of the plating temperature for the substrates fabricated by the PSL method (■) and by the PML method (▲).

as mentioned above. It is expected that the roughness of these originally prescribed Sn-seedless regions would also increase along with the plating time. Indeed, the variation of the surface roughness of these "Sn-seedless" (unstamped) regions as a function of the plating time is shown in Figure 10. The surface roughness of the Sn-seedless (OTS-SAM masking layer) regions for the PML method only slightly increases along with the plating time, as shown in Figure 10 for comparison. That indicates that the PML method has better selectivity of silver deposition than the PSL method. In other words, the OTS-SAM masking layer (by the PML method) has much better anti-adhesion of the Sn-catalyst and deposited silver than the bare glass (by the PSL method).

Note that all of the results mentioned above are carried out at a fixed temperature 45 °C. Now we would like to further explore the temperature effect on the electroless silver plating. Figure 11 shows the variation of the thickness of the deposited silver pattern as a function of the plating temperature at a fixed plating time of 4 min by using the PSL and PML methods. The silver thickness monotonically increases along with the plating temperature. That is, the growth rate is higher at higher temperatures. The surface roughness in the silver pattern regions

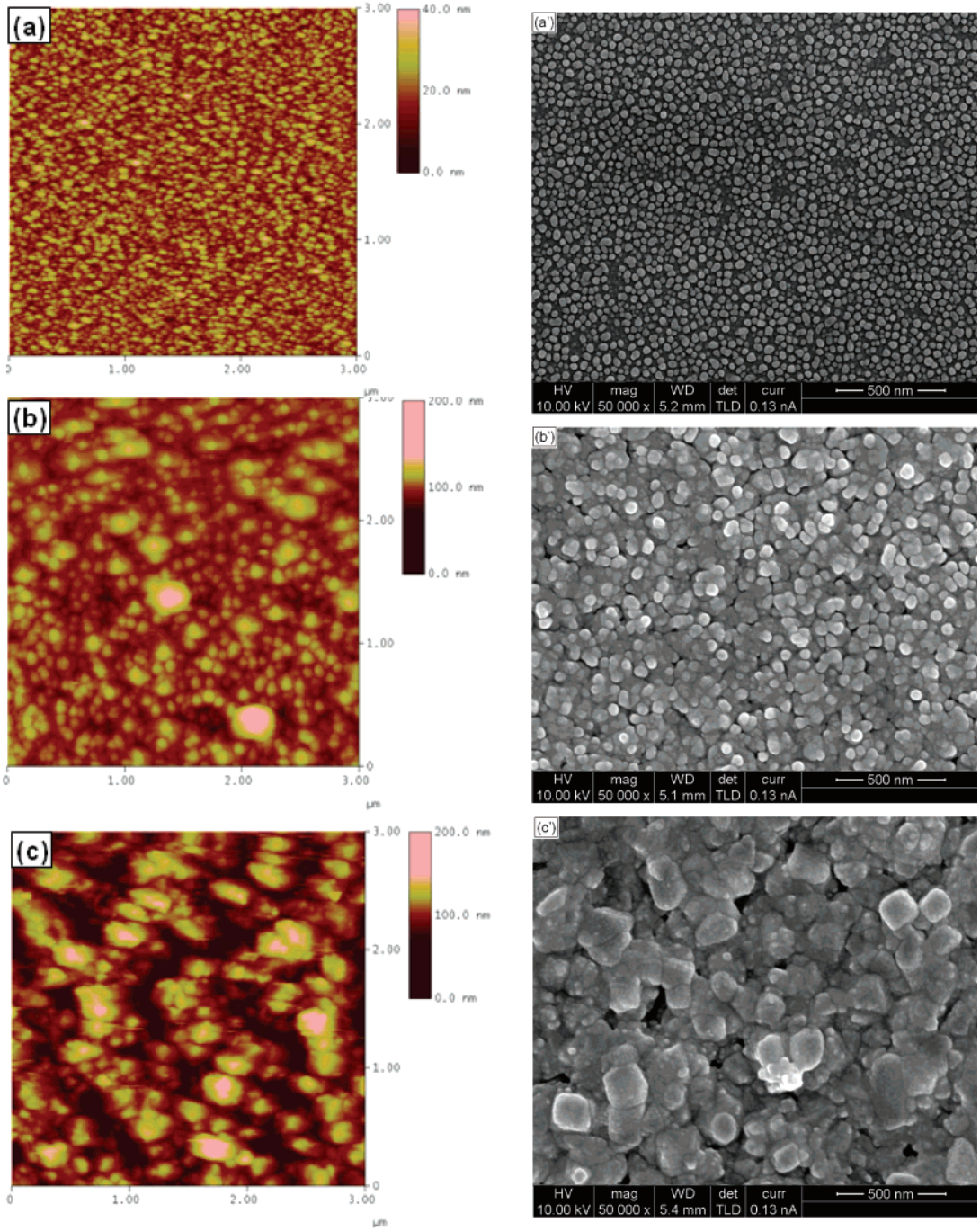


**Figure 12.** AFM (left column) and SEM (right column) images of silver pattern under the condition of a fixed plating time of 4 min at 25 °C (a and a′), 45 °C (b and b′), and 65 °C (c and c′). AFM image size: 3 $\mu$m × 3 $\mu$m. The substrates are fabricated by the PML method.

also becomes greater at higher temperatures, as shown in Figure 11. Figure 12 presents the AFM and SEM images to illustrate the plating temperature effect on the morphology of the deposited silver pattern prepared at 25, 45, and 65 °C. It is obvious that the silver grain size increases along with an increase in the plating temperature at a fixed plating time of 4 min. At the plating temperature of 25 °C, the silver grain size is around 56(±6) nm. Recall that the grain size is increased to 138(±17) nm for the plating temperature of 45 °C. The grain size is further increased up to 288(±101) nm at the plating temperature of 65 °C. The variation of the grain size increases along with the plating temperature. Especially, the standard deviation of the grain size is as large as 101 nm for the plating temperature of 65 °C due to poor stability of the plating solution at high temperatures. In addition, the grain is in round shape at low temperature (25 °C), as shown in Figure 12a′, and the grain becomes more square-like at high-temperature (65 °C), as shown in Figure 12c′.

It should be noted that the silver plating solution becomes unstable and cloudy when the plating temperature is high. Especially when the plating temperature is above 55 °C, the plating solution can hardly last for more than 5 min. According to our experimental results, the suitable plating temperature is below 45 °C for the plating solution used in this study.

## 4. Conclusion

Two methods of fabrication of silver pattern on glass substrates are proposed by using a combination of $\mu$CP and electroless plating. (1) The PSL method is to pattern the catalyst Sn directly via $\mu$CP. (2) The PML method is to apply $\mu$CP to pattern OTS-

SAM as a protection layer first and then the immersion of the OTS-SAM patterned substrate to deposit catalyst Sn on the unstamped areas. Both methods have very good selectivity for the electroless silver plating. Yet, more precisely, the deposited silver pattern fabricated by the PML method has slightly better selectivity than that of the PSL method. The OTS-SAM has an excellent property of anti-adhesion of deposited silver. Lateral dimensions easily reach the feature size of 0.6 $\mu$m in this study, and an extension into the smaller feature sizes is straightforward.[19,20] Note that the lateral diffusion of printing molecules could be carefully resolved for even smaller feature sizes.[21]

LA7023988

(19) Xia, Y. N.; Whitesides, G. M. *J. Am. Chem. Soc.* **1995**, *117*, 3274.
(20) Delamarche, E.; Schmid, H.; Bietsch, A.; Larsen, N. B.; Rithuizen, H.; Michel, B.; Biebuyck, H. *J. Phys. Chem. B* **1998**, *102*, 3324.
(21) Sharpe, R. B. A.; Burdinski, D.; Huskens, J.; Zandvliet, H. J. W.; Reinhoudt, D. N.; Poelsema, B. *Langmuir* **2004**, *20*, 8646.